J. Nonlinear Funct. Anal. 2022 (2022), Article ID 39 https://doi.org/10.23952/jnfa.2022.39

Journal of Nonlinear Functional Analysis
Available online at http://jnfa.mathres.org

A CHARACTERISTIC MIXED FINITE ELEMENT METHOD FOR BILINEAR CONVECTION-DIFFUSION OPTIMAL CONTROL PROBLEMS

YUELONG TANG

College of Science, Hunan University of Science and Engineering, Yongzhou 425100, China

Abstract. In this paper, we investigate a fully discrete characteristic mixed finite element approximation of bilinear convection-diffusion optimal control problems. The characteristic line method and backward difference are used for the time discretization. The lowest order Raviart-Thomas mixed finite element method is used for the space discretization. A priori error estimates for both the control and state numerical solutions are derived. Theoretical results are confirmed by a numerical example.

Keywords. A priori error estimates; Bilinear convection-diffusion optimal control problems; Characteristic mixed finite element methods.

1. Introduction

There are numerous studies on mixed finite element methods (MFEMs) for standard elliptic and parabolic optimal control problems (OCPs), in which the objective functional contains not only the primal state variable but also its gradient. A systematic introduction can be found in [1, 3, 13, 17, 18, 19, 20]. A priori error estimates of the MFEM for linear and semilinear elliptic OCPs were established in [4] and [14], respectively. A priori error estimates of the MFEM for linear and semilinear parabolic OCPs were derived in [27] and [5], respectively. In recent years, a priori error estimates of the MFEM for bilinear optimal control problems governed by elliptic and parabolic PDEs were obtained in [6] and [21], respectively.

Time-dependent convection-diffusion partial differential equations (PDEs) arise in groundwater contaminant transport, environmental modeling, petroleum reservoir simulation, and many other applications [22, 26, 29]. But convection dominated will produce unacceptable nonphysical oscillations of standard finite difference or finite element solutions. In order to overcome this difficulty, Douglas and Russell presented a characteristic finite element method (CFEM) of the convection-dominated diffusion problems in [7]. Recently, it was extended to solve other

E-mail address: tangyuelonga@163.com.
Received June 2, 2022; Accepted September 6, 2022.

convection-diffusion equations [23, 28] and linear convection-diffusion optimal control problems (CDOCPs) [8, 9, 10, 12, 24]. In [11], the authors derived the convergence results of characteristic mixed finite element methods (CMFEMs) for linear CDOCPs.

To the best of our knowledge, this is the first time to consider a fully discrete CMFEM approximation of bilinear OCPs governed by unsteady convection-diffusion equations. In this paper, we adopt the standard notation $W^{m,p}(\Omega)$ for Sobolev spaces on Ω with a norm $\|v\|_{m,p}^p = \sum\limits_{|\alpha|\leq m} \|D^\alpha v\|_{L^p(\Omega)}^p$, a semi-norm $|v|_{m,p}^p = \sum\limits_{|\alpha|=m} \|D^\alpha v\|_{L^p(\Omega)}^p$. We set $W_0^{m,p}(\Omega) = \{v \in W^{m,p}(\Omega) : v|_{\partial\Omega} = 0\}$. For $p=2$, let $H^m(\Omega) = W^{m,2}(\Omega)$, $H_0^m(\Omega) = W_0^{m,2}(\Omega)$, and $\|\cdot\|_m = \|\cdot\|_{m,2}$, $\|\cdot\| = \|\cdot\|_{0,2}$. We denote by $L^s(0,T;W^{m,p}(\Omega))$ the Banach space of all L^s integrable functions from J into $W^{m,p}(\Omega)$ with norm

$$\|v\|_{L^s(J;W^{m,p}(\Omega))} = \left(\int_0^T ||v||_{W^{m,p}(\Omega)}^s dt \right)^{\frac{1}{s}} \text{ for } s \in [1, \infty),$$

and the standard modification for $s = \infty$.

We are interested in the following time-dependent bilinear convection-diffusion OCPs:

$$\begin{cases} \min\limits_{u \in K} \dfrac{1}{2} \displaystyle\int_0^T \left(\|\boldsymbol{p} - \boldsymbol{p}_d\|^2 + \|y - y_d\|^2 + \|u\|^2 \right) dt, \\ y_t + \boldsymbol{b} \cdot \nabla y + \mathrm{div}\boldsymbol{p} + uy = f, \quad (x,t) \in \Omega \times J, \\ \boldsymbol{p} = -A\nabla y, \quad (x,t) \in \Omega \times J, \\ y(x,t) = 0, \quad (x,t) \in \partial\Omega \times J, \\ y(x,0) = y_0(x), \quad x \in \Omega, \end{cases} \tag{1.1}$$

where $\Omega \subset \mathbf{R}^2$ is a bounded convex polygon with Lipschitz boundary $\partial\Omega$ and $J = (0,T]$. Let $\boldsymbol{p}_d \in (L^2(J;H^1(\Omega)))^2$, $y_d \in L^2(J;H^1(\Omega))$, and $A = (a_{ij}(x))_{2\times 2} \in (W^{1,\infty}(\bar{\Omega}))^{2\times 2}$ such that $\mathbf{x}^T A \mathbf{x} > c\|\mathbf{x}\|_{\mathbf{R}^2}^2, \forall\, \mathbf{x} \in \mathbf{R}^2$, where $c > 0$, $f \in L^2(J;L^2(\Omega))$, and $y_0(x) \in H_0^1(\Omega)$. $\boldsymbol{b} = (b_1, b_2) \in (C(J;C_0^1(\bar{\Omega})))^2$ denotes a velocity field and the flow is incompressible, i.e.,

$$\nabla \cdot \boldsymbol{b} = 0, \forall (x,t) \in \Omega \times J.$$

Moreover, we assume that the constraint is an obstacle such that

$$K = \left\{ u \in L^\infty(J;L^2(\Omega)) :\ u(x,t) \geq 0, \text{ a.e. in } \Omega \times J \right\}.$$

Similarly, one can define the spaces $H^l(J;W^{m,p}(\Omega))$. Just for simplicity of statement, we denote $L^s(J;W^{m,p}(\Omega))$ by $L^s(W^{m,p})$. In addition, C denotes a general positive constant.

The rest of the paper is organized as follows. In Section 2, we give a fully discrete CMFEM approximation of OCPs (1.1). In Section 3, we introduce some important intermediate variables and error estimates. In Section 4, we derive a priori error estimates for both the control and state variables. In Section 5, the last section, a numerical example is provided to demonstrate that the proposed method is efficient.

2. A Characteristic Mixed Finite Element Approximation

We give a fully discrete CMFEM for model problem (1.1). To fix the idea, we take the state spaces $\boldsymbol{L} = L^2(J;\boldsymbol{V})$ and $Q = H^1(J;W)$, where $\boldsymbol{V}$ and W are defined as follows:

$$\boldsymbol{V} = H(\mathrm{div};\Omega) = \left\{ \boldsymbol{v} \in (L^2(\Omega))^2, \mathrm{div}\boldsymbol{v} \in L^2(\Omega) \right\}, W = L^2(\Omega).$$

The Hilbert space $\boldsymbol{V}$ is equipped with the following norm:

$$\|\boldsymbol{v}\|_{H(\mathrm{div};\Omega)}=\left(\|\boldsymbol{v}\|_{0,\Omega}^2+\|\mathrm{div}\boldsymbol{v}\|_{0,\Omega}^2\right)^{1/2}.$$

Let s denote the unit vector in the direction of $(b_1,b_2,1)$ in $\Omega\times J$, and

$$\lambda=\left(|\boldsymbol{b}|^2+1\right)^{1/2}=\left(b_1^2+b_2^2+1\right)^{1/2}.$$

We take account of $y_t+\boldsymbol{b}\cdot\nabla y$ as a directional derivative, namely

$$y_t+\boldsymbol{b}\cdot\nabla y=\lambda y_s.$$

Then the state equation is equivalent to the following form:

$$\lambda y_s+\mathrm{div}\boldsymbol{p}+uy=f.$$

We recast (1.1) as the following weak form:

$$\begin{cases}\min\limits_{u\in K}\left\{\dfrac{1}{2}\displaystyle\int_0^T\left(\|\boldsymbol{p}-\boldsymbol{p}_d\|^2+\|y-y_d\|^2+\|u\|^2\right)dt\right\},\\(\lambda y_s,w)+(\mathrm{div}\boldsymbol{p},w)+(uy,w)=(f,w),\quad\forall w\in W,\ t\in J,\\(A^{-1}\boldsymbol{p},\boldsymbol{v})-(y,\mathrm{div}\boldsymbol{v})=0,\quad\forall\boldsymbol{v}\in\boldsymbol{V},\ t\in J,\\y(x,0)=y_0(x),\quad\forall x\in\Omega.\end{cases}\tag{2.1}$$

It follows from [2, 9, 18] that the OCP (2.1) has a solution $(\boldsymbol{p},y,u)$, and that if $(\boldsymbol{p},y,u)\in\boldsymbol{L}\times Q\times K$ is a solution of (2.1), then there is a co-state $(\boldsymbol{q},z)\in\boldsymbol{L}\times Q$ such that $(\boldsymbol{p},y,\boldsymbol{q},z,u)$ satisfies the following optimality conditions:

$$(\lambda y_s,w)+(\mathrm{div}\boldsymbol{p},w)+(uy,w)=(f,w),\quad\forall w\in W,\ t\in J,\tag{2.2}$$

$$(A^{-1}\boldsymbol{p},\boldsymbol{v})-(y,\mathrm{div}\boldsymbol{v})=0,\quad\forall\boldsymbol{v}\in\boldsymbol{V},\ t\in J,\tag{2.3}$$

$$y(x,0)=y_0(x),\quad\forall x\in\Omega,\tag{2.4}$$

$$-(\lambda p_s,w)+(\mathrm{q},w)+(uz,w)=(y-y_d,w),\quad\forall w\in W,\ t\in J,\tag{2.5}$$

$$(A^{-1}\boldsymbol{q},\boldsymbol{v})-(z,\mathrm{div}\boldsymbol{v})=-(\boldsymbol{p}-\boldsymbol{p}_d,\boldsymbol{v}),\quad\forall\boldsymbol{v}\in\boldsymbol{V},\ t\in J,\tag{2.6}$$

$$z(x,T)=0,\quad\forall x\in\Omega,\tag{2.7}$$

$$(u-yz,\tilde{u}-u)\geq 0,\quad\forall\tilde{u}\in K,\tag{2.8}$$

where $(\cdot,\cdot)$ is the inner product of $L^2(\Omega)$.

Let $N\in\mathbb{Z}^+$, $0=t_1\leq t_2\leq\cdots\leq t_N=T$, $k_n=t_n-t_{n-1},n=1,2,\cdots,N$, $k=\max\limits_{1\leq n\leq N}\{k_n\}$ and

$$G(x^*,t^*;t)=x^*-\boldsymbol{b}(x^*,t^*)(t^*-t)$$

be the approximate characteristic curve passing through point x^* at time t^*. Furthermore, we denote by $\bar{x}=G(x,t_n;t_{n-1})$ be the foot at time t_{n-1} of the characteristic curve with head x at time t_n and set $\bar{\psi}=\psi(\bar{x},t)$, $\psi^n=\psi(x,t_n)$. Then we approximate the s derivative of y at time t_n by a backward-Euler difference quotient, namely

$$\lambda^n y_s^n\simeq\frac{y^n-\bar{y}^{n-1}}{k_n},\ n=1,2,\cdots,N.$$

We define for $1 \le p < \infty$ the discrete time-dependent norms

$$|||\psi|||_{l^p(J;W^{m,q}(\Omega))} := \left(\sum_{n=1-l}^{N-l} k_n \|\psi^n\|^p_{W^{m,q}(\Omega)} \right)^{\frac{1}{p}},$$

where $l = 0$ for the control u and the state $y, \boldsymbol{p}$ and $l = 1$ for the adjoint state $z, \boldsymbol{q}$, with the standard modification for $p = \infty$. For convenience, we denote $|||\cdot|||_{l^p(J;W^{m,q}(\Omega))}$ by $|||\cdot|||_{l^p(W^{m,q})}$ and let $l^p(J;W^{m,q}(\Omega)) := \left\{\psi : |||\psi|||_{l^p(W^{m,q})} < \infty\right\}, 1 \le p \le \infty$.

Let $\mathscr{T}_h$ be regular triangulations of Ω. h_τ is the diameter of element τ and $h = \max_{\tau \in \mathscr{T}_h}\{h_\tau\}$. Let $\boldsymbol{V}_h \times W_h \subset \boldsymbol{V} \times W$ denote the lowest order Raviart-Thomas space [1] associated with the triangulations $\mathscr{T}_h$ of Ω. P_k denotes the space of polynomials of total degree at most k ($k \ge 0$). Let $\boldsymbol{V}(\tau) = \{\boldsymbol{v} \in P_0^2(\tau) + x \cdot P_0(\tau)\}$, $W(\tau) = P_0(\tau)$. We define

$$\begin{aligned}
\boldsymbol{V}_h &:= \{\boldsymbol{v}_h \in \boldsymbol{V} : \boldsymbol{v}_h|_\tau \in \boldsymbol{V}(\tau), \forall\, \tau \in \mathscr{T}_h\},\\
W_h &:= \{w_h \in W : w_h|_\tau \in W(\tau), \forall\, \tau \in \mathscr{T}_h\},\\
K_h &:= \{w_h \in W_h : w_h|_\tau = \max\{0, w_h\}, \forall\, \tau \in \mathscr{T}_h\}.
\end{aligned}$$

We introduce the $L^2(\Omega)$-orthogonal projection [1] $P_h : W \to W_h$, which satisfies:

$$(P_h\psi - \psi, w_h) = 0, \qquad \forall w_h \in W_h, \forall \psi \in W,$$

and the Fortin projection [6] $\Pi_h : \boldsymbol{V} \to \boldsymbol{V}_h$, which satisfies:

$$(\mathrm{div}\,(\Pi_h\boldsymbol{\psi} - \boldsymbol{\psi}), w_h) = 0, \qquad \forall w_h \in W_h, \forall \boldsymbol{\psi} \in \boldsymbol{V}.$$

They have the following approximation properties [1]:

$$\|\psi - P_h\psi\|_{-s,\rho} \le Ch^{1+s}\|\psi\|_{1,\rho}, s = 0,1,2 \le \rho \le \infty, \forall \psi \in W^{1,\rho}(\Omega), \tag{2.9}$$

$$\|\boldsymbol{\psi} - \Pi_h\boldsymbol{\psi}\|_{0,\rho} \le Ch\|\boldsymbol{\psi}\|_{1,\rho}, 2 \le \rho \le \infty, \forall \boldsymbol{\psi} \in \left(W^{1,\rho}(\Omega)\right)^2. \tag{2.10}$$

Then a fully discrete CMFEM approximation of (2.1) is as follows:

$$\begin{cases}
\min\limits_{u_h^n \in K_h} \left\{ \dfrac{1}{2} \displaystyle\sum_{n=1}^{N} k_n \left(\|\boldsymbol{p}_h^n - \boldsymbol{p}_d^n\|^2 + \|y_h^n - y_d^n\|^2 + \|u_h^n\|^2 \right) \right\}\\
\left(\dfrac{y_h^n - \bar{y}_h^{n-1}}{k_n}, w_h \right) + (\mathrm{div}\boldsymbol{p}_h^n, w_h) + (u_h^n y_h^n, w_h) = (f^n, w_h), \quad \forall w_h \in W_h,\\
(A^{-1}\boldsymbol{p}_h^n, \boldsymbol{v}_h) - (y_h^n, \mathrm{div}\boldsymbol{v}_h) = 0, \quad \forall \boldsymbol{v}_h \in \boldsymbol{V}_h,\\
y_h^0(x) = P_h y_0(x), \quad \forall x \in \Omega.
\end{cases} \tag{2.11}$$

It follows from [2, 9, 25] that control problem (2.11) has a solution $(\boldsymbol{p}_h^n, y_h^n, u_h^n), n = 1,2,\cdots,N$, and that if $(\boldsymbol{p}_h^n, y_h^n, u_h^n) \in \boldsymbol{V}_h \times W_h \times K_h$ is the solution of (2.11), then, for $n = N, N-1, \cdots, 1$, there is a co-state $(\boldsymbol{q}_h^{n-1}, z_h^n) \in \boldsymbol{V}_h \times W_h$ such that $(\boldsymbol{p}_h^n, y_h^n, \boldsymbol{q}_h^{n-1}, z_h^{n-1}, u_h^n)$ satisfies the following optimality conditions:

$$\left(\frac{y_h^n-\bar{y}_h^{n-1}}{k_n},w_h\right)+(\mathrm{div}\boldsymbol{p}_h^n,w_h)+(u_h^ny_h^n,w_h)=(f^n,w_h),\quad \forall w_h\in W_h, \tag{2.12}$$

$$(A^{-1}\boldsymbol{p}_h^n,\boldsymbol{v}_h)-(y_h^n,\mathrm{div}\boldsymbol{v}_h)=0,\quad \forall \boldsymbol{v}_h\in \boldsymbol{V}_h, \tag{2.13}$$

$$y_h^0(x)=R_hy_0(x),\quad \forall x\in\Omega, \tag{2.14}$$

$$\left(\frac{z_h^{n-1}-\bar{\bar{z}}_h^n\cdot J^n}{k_n},w_h\right)+(\mathrm{div}\boldsymbol{q}_h^{n-1},w_h)+(u_h^nz_h^{n-1},w_h)=(y_h^n-y_d^n,w_h),\quad \forall w_h\in W_h, \tag{2.15}$$

$$(A^{-1}\boldsymbol{q}_h^{n-1},\boldsymbol{v}_h)-(z_h^{n-1},\mathrm{div}\boldsymbol{v}_h)=-(\boldsymbol{p}_h^n-\boldsymbol{p}_d^n,\boldsymbol{v}_h),\quad \forall \boldsymbol{v}_h\in \boldsymbol{V}_h, \tag{2.16}$$

$$z_h^N(x)=0,\quad \forall x\in\Omega, \tag{2.17}$$

$$(u_h^n-y_h^nz_h^{n-1},\tilde{u}-u_h^n)\geq 0,\quad \forall \tilde{u}\in K_h. \tag{2.18}$$

where $\bar{\bar{z}}_h^n=z_h(\bar{\bar{x}},t_n)$ and $\bar{\bar{x}}$ represents the head of the characteristic curve with foot x at time t_{n-1}, namely,

$$x=G(\bar{\bar{x}},t_n;t_{n-1}),$$

and $J^n=\det\,\mathscr{D}G(x,t_n;t_{n-1})^{-1}$ is the determinant of the Jacobian transformation from G to x. Because the flow is incompressible, similar to the discussion in [9], we have $J^n=1+O(k_n^2)$.

3. Some Important Intermediate Variables and Error Estimates

We introduce some auxiliary variables and error estimates. For any $u\in K, n=1,2,\cdots,N$, let $\big(\boldsymbol{p}_h^n(u),y_h^n(u),\boldsymbol{q}_h^{n-1}(u),z_h^{n-1}(u)\big)\in(\boldsymbol{V}_h\times W_h)^2$ satisfy the following system:

$$\left(\frac{y_h^n(u)-\bar{y}_h^{n-1}(u)}{k_n},w_h\right)+(\mathrm{div}\boldsymbol{p}_h^n(u),w_h)+(u^ny_h^n(u),w_h)=(f^n,w_h),\quad \forall w_h\in W_h, \tag{3.1}$$

$$(A^{-1}\boldsymbol{p}_h^n(u),\boldsymbol{v}_h)-(y_h^n(u),\mathrm{div}\boldsymbol{v}_h)=0,\quad \forall \boldsymbol{v}_h\in \boldsymbol{V}_h, \tag{3.2}$$

$$y_h^0(u)=P_hy_0(x),\quad \forall x\in\Omega, \tag{3.3}$$

$$\begin{aligned}&\left(\frac{z_h^{n-1}(u)-\bar{\bar{z}}_h^n(u)\cdot J^n}{k_n},w_h\right)+(\mathrm{div}\boldsymbol{q}_h^{n-1}(u),w_h)+(u^nz_h^{n-1}(u),w_h)\\&=(y_h^n(u)-y_d^n,w_h),\quad \forall w_h\in W_h,\end{aligned} \tag{3.4}$$

$$(A^{-1}\boldsymbol{q}_h^{n-1}(u),\boldsymbol{v}_h)-(z_h^{n-1}(u),\mathrm{div}\boldsymbol{v}_h)=-(\boldsymbol{p}_h^n(u)-\boldsymbol{p}_d^n,\boldsymbol{v}_h),\quad \forall \boldsymbol{v}_h\in \boldsymbol{V}_h, \tag{3.5}$$

$$z_h^N(u)=0,\quad \forall x\in\Omega. \tag{3.6}$$

It is easy to see that $\big(\boldsymbol{p}_h^n,y_h^n,\boldsymbol{q}_h^{n-1},z_h^{n-1}\big)=\big(\boldsymbol{p}_h^n(u_h),y_h^n(u_h),\boldsymbol{q}_h^{n-1}(u_h),z_h^{n-1}(u_h)\big)$. For simplicity of presentation, we set

$$\begin{aligned}\eta^n=y_h^n-y_h^n(u),\boldsymbol{\theta}^n=\boldsymbol{p}_h^n-\boldsymbol{p}_h^n(u),\zeta^n=z_h^n-z_h^n(u),\boldsymbol{\xi}^n=\boldsymbol{q}_h^n-\boldsymbol{q}_h^n(u),\\ \rho^n=y^n-y_h^n(u),\boldsymbol{\sigma}^n=\boldsymbol{p}^n-\boldsymbol{p}_h^n(u),\mu^n=z^n-z_h^n(u),\boldsymbol{\nu}^n=\boldsymbol{q}^n-\boldsymbol{q}_h^n(u),\end{aligned}$$

where $n=0,1,\cdots,N$.

The following lemmas are very important in convergence analysis.

Lemma 3.1. [7] *Suppose that $f \in L^2(\Omega)$ and $\bar{f}(x) = f(x+g(x)k)$, where g and g' are bounded. Then*

$$\|f(x)-\bar{f}(x)\|_{-1} \leq Ck\|f\|. \tag{3.7}$$

Lemma 3.2. *Let $n = 1,2,\cdots,N$, $\left(\boldsymbol{p}_h^n, y_h^n, \boldsymbol{q}_h^{n-1}, z_h^{n-1}, u_h^n\right)$, and $\left(\boldsymbol{p}_h^n(u), y_h^n(u), \boldsymbol{q}_h^{n-1}(u), z_h^{n-1}(u)\right)$ be the solutions to (2.12)-(2.18) and (3.1)-(3.6), respectively. Then the following estimates hold*

$$|||y_h - y_h(u)|||_{l^\infty(L^2)} + |||\boldsymbol{p}_h - \boldsymbol{p}_h(u)|||_{l^2(L^2)} \leq C\left(k + |||u-u_h|||_{l^2(L^2)}\right),$$
$$|||z_h - z_h(u)|||_{l^\infty(L^2)} + |||\boldsymbol{q}_h - \boldsymbol{q}_h(u)|||_{l^2(L^2)} \leq C\left(k + |||u-u_h|||_{l^2(L^2)}\right).$$

Proof. From (2.12)-(2.13) and (3.1)-(3.2), we have

$$\begin{aligned} &\left(\frac{\eta^n-\eta^{n-1}}{k_n}, w_h\right) + (\mathrm{div}\boldsymbol{\theta}^n, w_h) + (u^n\eta^n, w_h) \\ &= ((u^n-u_h^n)y_h^n, w_h) + \left(\frac{\bar{\eta}^{n-1}-\eta^{n-1}}{k_n}, w_h\right), \quad \forall w_h \in W_h, \end{aligned} \tag{3.8}$$

$$(A^{-1}\boldsymbol{\theta}^n, \boldsymbol{v}_h) - (\eta^n, \mathrm{div}\boldsymbol{v}_h) = 0, \quad \forall \boldsymbol{v}_h \in \boldsymbol{V}_h. \tag{3.9}$$

From the inequality $a(a-b) \geq \frac{a^2-b^2}{2}$, we have

$$\frac{\|\eta^n\|^2 - \|\eta^{n-1}\|^2}{2k_n} \leq \left(\frac{\eta^n-\eta^{n-1}}{k_n}, \eta^n\right). \tag{3.10}$$

In view of $u \in K$, we have

$$(u^n\eta^n, \eta^n) \geq 0. \tag{3.11}$$

It follows from Lemma 3.1 and the Cauchy inequality with ε that

$$((u^n-u_h^n)y_h^n, \eta^n) \leq C(\varepsilon)\|u^n-u_h^n\|^2\|y_h^n\|_1^2 + \varepsilon\|\eta^n\|_1^2, \tag{3.12}$$

and

$$\left(\frac{\bar{\eta}^{n-1}-\eta^{n-1}}{k_n}, \eta^n\right) \leq \frac{\|\bar{\eta}^{n-1}-\eta^{n-1}\|_{-1}\|\eta^n\|_1}{k_n} \leq C(\varepsilon)k_n^2\|\eta^{n-1}\|^2 + \frac{\varepsilon}{k_n^2}\|\eta^n\|_1^2. \tag{3.13}$$

Set $w_h = \eta^n$ and $\boldsymbol{v}_h = \boldsymbol{\theta}^n$ in (3.8) and (3.9), respectively. From (3.8)-(3.13), we obtain

$$\begin{aligned} &\frac{\|\eta^n\|^2 - \|\eta^{n-1}\|^2}{2k_n} + c\|\boldsymbol{\theta}^n\|^2 \\ &\leq C(\varepsilon)\|u^n-u_h^n\|^2 + \varepsilon\|\eta^n\|^2 + C(\varepsilon)k_n^2\|\eta^{n-1}\|^2 + \frac{\varepsilon}{k_n^2}\|\eta^n\|_1^2. \end{aligned} \tag{3.14}$$

Note that $\eta^0 = 0$ and $\|\eta^n\|_1 \leq C\|\boldsymbol{\theta}^n\|$. By multiplying both sides of (3.14) by $2k_n$ and summing over n from 1 to N, we derive

$$|||\eta|||_{l^\infty(L^2)} + |||\boldsymbol{\theta}|||_{l^2(L^2)} \leq C\left(k + |||u_h-u|||_{l^2(L^2)}\right). \tag{3.15}$$

Similarly, it follows from (2.15)-(2.16) and (3.4)-(3.5) that

$$\begin{aligned}
&\left(\frac{\zeta^{n-1}-\zeta^n}{k_n}, w_h\right)+\left(\operatorname{div}\boldsymbol{\xi}^{n-1}, w_h\right)+\left(u^n\zeta^{n-1}, w_h\right)\\
&=\left(\eta^n, w_h\right)+\left((u^n-u_h^n)z_h^{n-1}, w_h\right)+\left(\frac{\bar{\bar{\zeta}}^n-\zeta^n}{k_n}, w_h\right)\\
&\quad+\left(\frac{\bar{\bar{\zeta}}^n\cdot J^n-\bar{\bar{\zeta}}^n}{k_n}, w_h\right), \ \forall w_h\in W_h,
\end{aligned} \tag{3.16}$$

$$\left(A^{-1}\boldsymbol{\xi}^{n-1}, \boldsymbol{v}_h\right)-\left(\zeta^{n-1}, \operatorname{div}\boldsymbol{v}_h\right)=-\left(\boldsymbol{\theta}^n, \boldsymbol{v}_h\right), \qquad \forall \boldsymbol{v}_h\in \boldsymbol{V}_h. \tag{3.17}$$

By choosing $w_h=\zeta^{n-1}$ and $\boldsymbol{v}_h=\boldsymbol{\xi}^{n-1}$ in (3.16) and (3.17) respectively, we can derive the desired conclusion. □

Lemma 3.3. *Let* $(\boldsymbol{p}, y, \boldsymbol{q}, z, u)$ *and* $\left(\boldsymbol{p}_h^n(u), y_h^n(u), \boldsymbol{q}_h^{n-1}(u), z_h^{n-1}(u)\right), n=1,2,\cdots,N$ *be the solutions of (2.2)-(2.8) and (3.1)-(3.6), respectively. Assume that* $y,z\in L^\infty(H_0^1)\cap L^\infty(H^2)\cap H^1(H^1)\cap H^2(L^2)$ *and* $\boldsymbol{p},\boldsymbol{q}\in (L^2(H^1))^2\cap(H^1(L^2))^2$. *Then the following estimates hold*

$$|||y-y_h(u)|||_{l^\infty(L^2)}+|||\boldsymbol{p}-\boldsymbol{p}_h(u)|||_{l^2(L^2)}\le C(k+h), \tag{3.18}$$

$$|||z-z_h(u)|||_{l^\infty(L^2)}+|||\boldsymbol{q}-\boldsymbol{q}_h(u)|||_{l^2(L^2)}\le C(k+h). \tag{3.19}$$

Proof. It follows from (2.2)-(2.3) and (3.1)-(3.2) that

$$\begin{aligned}
&\left(\frac{\rho^n-\rho^{n-1}}{k_n}, w_h\right)+\left(\operatorname{div}\boldsymbol{\sigma}^n, w_h\right)+\left(u^n\rho^n, w_h\right)\\
&=\left(\frac{\bar{\rho}^{n-1}-\rho^{n-1}}{k_n}, w_h\right)+\left(\frac{y^n-\bar{y}^{n-1}}{k_n}-\lambda^n y_s^n, w_h\right), \quad \forall w_h\in W_h,
\end{aligned} \tag{3.20}$$

$$\left(A^{-1}\boldsymbol{\sigma}^n, \boldsymbol{v}_h\right)-\left(\rho^n, \operatorname{div}\boldsymbol{v}_h\right)=0, \qquad \forall \boldsymbol{v}_h\in \boldsymbol{V}_h. \tag{3.21}$$

According to (3.20)-(3.21) and the definitions of projections P_h and Π_h, we have

$$\begin{aligned}
&\left(\frac{\rho^n-\rho^{n-1}}{k_n}, \rho^n\right)+\left(A^{-1}\boldsymbol{\sigma}^n, \boldsymbol{\sigma}^n\right)+\left(u^n\rho^n, \rho^n\right)\\
&=\left(\frac{\rho^n-\rho^{n-1}}{k_n}, y^n-P_hy^n\right)+\left(A^{-1}\boldsymbol{\sigma}^n, \boldsymbol{p}^n-\Pi_h\boldsymbol{p}^n\right)+\left(u^n\rho^n, \rho^n\right)\\
&\quad+\left(\frac{\rho^n-\rho^{n-1}}{k_n}, P_hy^n-y_h^n(u)\right)+\left(\operatorname{div}(\boldsymbol{p}^n-\boldsymbol{p}_h^n(u)), P_hy^n-y_h^n(u)\right)\\
&=\left(\frac{\rho^n-\rho^{n-1}}{k_n}, y^n-P_hy^n\right)+\left(A^{-1}\boldsymbol{\sigma}^n, \boldsymbol{p}^n-\Pi_h\boldsymbol{p}^n\right)+\left(u^n\rho^n, y^n-P_hy^n\right)\\
&\quad+\left(\frac{\bar{\rho}^{n-1}-\rho^{n-1}}{k_n}, P_hy^n-y_h^n(u)\right)+\left(\frac{y^n-\bar{y}^{n-1}}{k_n}-\lambda^n y_s^n, P_hy^n-y_h^n(u)\right).
\end{aligned} \tag{3.22}$$

Similar to (3.10), we have

$$\frac{\|\rho^n\|^2-\|\rho^{n-1}\|^2}{2k_n}\le\left(\frac{\rho^n-\rho^{n-1}}{k_n}, \rho^n\right). \tag{3.23}$$

By using (2.9), Lemma 3.1 and Cauchy inequality, we have

$$\left(\frac{\bar{\rho}^{n-1}-\rho^{n-1}}{k_n}, y^n - P_h y^n\right) \le C\left(\frac{k_n}{2}+\frac{h^2}{2k_n}\right). \tag{3.24}$$

It follows from (2.10) and the Cauchy inequality with ε that

$$\left(A^{-1}\boldsymbol{\sigma}^n, \boldsymbol{p}^n - \Pi_h \boldsymbol{p}^n\right) \le C(\varepsilon)h^2 + \varepsilon\|\boldsymbol{\sigma}^n\|^2. \tag{3.25}$$

Note that $u \in K$. By utilizing (2.9) and the Cauchy inequality with ε, we obtain

$$(u^n\rho^n, y^n - P_h y^n) \le C(\varepsilon)h^2 + \varepsilon\|\rho^n\|^2. \tag{3.26}$$

It follows from (2.9), (3.7) and the Cauchy inequality with ε that

$$\begin{aligned}
&\left(\frac{\bar{\rho}^{n-1}-\rho^{n-1}}{k_n}, P_h y^n - y_h^n(u)\right)\\
&= \left(\frac{\bar{\rho}^{n-1}-\rho^{n-1}}{k_n}, P_h y^n - y^n + \rho^n\right)\\
&\le \frac{C}{k_n}\left(\|\bar{\rho}^{n-1}-\rho^{n-1}\|_{-1}\|P_h y^n - y^n\|_1 + \|\bar{\rho}^{n-1}-\rho^{n-1}\|_{-1}\|\rho^n\|_1\right)\\
&\le C(\varepsilon)k_n^2\|\rho^{n-1}\|^2 + \frac{\varepsilon C}{k_n^2}\left(h^2 + \|\rho^n\|_1^2\right).
\end{aligned} \tag{3.27}$$

From the standard backward difference error analysis [7] and the Cauchy inequality with ε, we obtain

$$\begin{aligned}
&\left(\frac{y^n-\bar{y}^{n-1}}{k_n} - \lambda^n y_s^n, P_h y^n - y_h^n(u)\right)\\
&\le C(\varepsilon)\left\|\frac{y^n-\bar{y}^{n-1}}{k_n} - \lambda^n y_s^n\right\|^2 + \varepsilon C\|P_h y^n - y^n + \rho^n\|^2\\
&\le C(\varepsilon)k_n\left\|\frac{\partial^2 y}{\partial s^2}\right\|^2_{L^2(t_{n-1},t_n;L^2(\Omega))} + \varepsilon C\left(h^4 + \|\rho^n\|^2\right).
\end{aligned} \tag{3.28}$$

Combining (3.22)-(3.28), we derive

$$\begin{aligned}
&\frac{\|\rho^n\|^2 - \|\rho^{n-1}\|^2}{2k_n} + c\|\boldsymbol{\sigma}^n\|^2\\
&\le C(\varepsilon)h^2 + C\left(\frac{k_n}{2}+\frac{h^2}{2k_n}\right) + \varepsilon(2\|\rho^n\|^2 + \|\rho^n\|_1^2 + \|\boldsymbol{\sigma}^n\|^2).
\end{aligned}$$

Multiply both sides of the above inequality by $2k_n$ and summing over n from 1 to N. If ε is small enough, we can obtain (3.18). Similarly, from (2.5)-(2.7) and (3.4)-(3.6) we can derive (3.19) immediately. □

4. A Priori Error Estimates

In many applications, the objective functional $J(\cdot,\cdot)$ is uniformly convex near the solution u. Like in [16], if h and k are small enough, we assume that there is a constant $c > 0$ such that

$$c|||u-u_h|||^2_{l^2(L^2)} \le (J'_{hk}(y_h,u) - J'_{hk}(y_h,u_h), u-u_h). \tag{4.1}$$

Theorem 4.1. *Let $(\boldsymbol{p},y,\boldsymbol{q},z,u)$ and $(\boldsymbol{p}_h^n,y_h^n,\boldsymbol{q}_h^{n-1},z_h^{n-1},u_h^n), n=1,2,\cdots,N$ be the solutions of (2.2)-(2.8) and (2.12)-(2.18), respectively. Let the conditions in lemmas 3.2-3.3 be valid and $u\in L^\infty(H^1)$. Then*

$$|||u-u_h|||_{l^2(L^2)}\leq C(h+k), \tag{4.2}$$

$$|||y-y_h|||_{l^\infty(L^2)}+|||\boldsymbol{p}-\boldsymbol{p}_h|||_{l^2(L^2)}\leq C(h+k), \tag{4.3}$$

$$|||z-z_h|||_{l^\infty(L^2)}+|||\boldsymbol{q}-\boldsymbol{q}_h|||_{l^2(L^2)}\leq C(h+k). \tag{4.4}$$

Proof. Selecting $\widetilde{u}=u_h$ and $\widetilde{u}=P_hu$ in (2.8) and (2.18), respectively, we have

$$(u^n-y^nz^n,u_h^n-u^n)\geq 0, \tag{4.5}$$

and

$$(u_h^n-y_h^nz_h^{n-1},P_hu^n-u_h^n)\geq 0. \tag{4.6}$$

According to the definition of P_h, (4.1), (4.5), and (4.6), we have

$$\begin{aligned}
&c|||u-u_h|||_{l^2(L^2)}^2\\
&\leq (J'_{hk}(y_h,u)-J'_{hk}(y_h,u_h),u-u_h)\\
&=\sum_{n=1}^N k_n\left(u^n-y_h^n(u)z_h^{n-1}(u),u^n-u_h^n\right)-\sum_{n=1}^N k_n\left(u_h^n-y_h^nz_h^{n-1},u^n-u_h^n\right)\\
&\leq \sum_{n=1}^N k_n\left(y^nz^n-y_h^n(u)z_h^{n-1}(u),u^n-u_h^n\right)+\sum_{n=1}^N k_n\left(u_h^n-y_h^nz_h^{n-1},P_hu^n-u^n\right)\\
&=\sum_{n=1}^N k_n\left(y^nz^{n-1}-y_h^n(u)z_h^{n-1}(u),u^n-u_h^n\right)+\sum_{n=1}^N k_n\left(y^nz^n-y^nz^{n-1},u^n-u_h^n\right)\\
&\quad+\sum_{n=1}^N k_n\left(y^nz^{n-1}-y_h^nz_h^{n-1},P_hu^n-u_h^n\right)+\sum_{n=1}^N k_n\left(P_h(y^nz^{n-1})-y^nz^{n-1},P_hu^n-u^n\right)\\
&:=I_1+I_2+I_3+I_4.
\end{aligned} \tag{4.7}$$

By using the Cauchy inequality with ε, we obtain

$$\begin{aligned}
I_1&=\sum_{n=1}^N k_n\left(y^nz^{n-1}-y_h^n(u)z_h^{n-1}(u),u^n-u_h^n\right)\\
&\leq C(\varepsilon)\sum_{n=1}^N k_n\|z^{n-1}-z_h^{n-1}(u)\|_1^2+C(\varepsilon)\sum_{n=1}^N k_n\|y^n-y_h^n(u)\|_1^2+\varepsilon C\sum_{n=1}^N k_n\|u^n-u_h^n\|^2\\
&=C(\varepsilon)|||z-z_h(u)|||_{l^2(H^1)}^2+C(\varepsilon)|||y-y_h(u)|||_{l^2(H^1)}^2+\varepsilon C|||u-u_h|||_{l^2(L^2)}^2,
\end{aligned} \tag{4.8}$$

and

$$\begin{aligned}
I_2&=\sum_{n=1}^N k_n\left(y^nz^n-y^nz^{n-1},u^n-u_h^n\right)\\
&\leq C(\varepsilon)\sum_{n=1}^N k_n\|z^n-z^{n-1}(u)\|_1^2+\varepsilon C\sum_{n=1}^N k_n\|u^n-u_h^n\|^2\\
&=C(\varepsilon)k^2|||p|||_{l^2(H^1)}^2+\varepsilon C|||u-u_h|||_{l^2(L^2)}^2.
\end{aligned} \tag{4.9}$$

It follows from the Cauchy inequality, (2.7), and Lemma 3.2 that

$$
\begin{aligned}
I_3 &= \sum_{n=1}^{N} k_n \left(y^n p^{n-1} - y_h^n p_h^{n-1}, P_h u^n - u_h^n\right) \\
&= \sum_{n=1}^{N} k_n \left(y^n p^{n-1} - y_h^n(u) p_h^{n-1}(u), P_h u^n - u_h^n\right) \\
&\quad + \sum_{n=1}^{N} k_n \left(y_h^n(u) p_h^{n-1}(u) - y_h^n p_h^{n-1}, P_h u^n - u_h^n\right) \\
&\leq C \sum_{n=1}^{N} k_n \|p^{n-1} - p_h^{n-1}(u)\|_1^2 + C \sum_{n=1}^{N} k_n \|y^{n-1} - y_h^{n-1}(u)\|_1^2 \\
&\quad + C \sum_{n=1}^{N} k_n \|u^n - P_h u^n\|^2 + \varepsilon C \left(k + |||u - u_h|||_{l^2(L^2)}^2\right) \\
&\leq C|||p - p_h(u)|||_{l^2(H^1)}^2 + C|||y - y_h(u)|||_{l^2(H^1)}^2 + Ch^2|||u|||_{l^2(H^1)}^2 \\
&\quad + \varepsilon C \left(k + |||u - u_h|||_{l^2(L^2)}^2\right),
\end{aligned} \tag{4.10}
$$

and

$$
\begin{aligned}
I_4 &= \sum_{n=1}^{N} k_n \left(P_h(y^n p^{n-1}) - y^n p^{n-1}, P_h u^n - u^n\right) \\
&\leq Ch^2 \left(|||y|||_{l^2(H^1)}^2 + |||p|||_{l^2(H^1)}^2 + |||u|||_{l^2(H^1)}^2\right).
\end{aligned} \tag{4.11}
$$

Combining (4.7)-(4.11), we obtain (4.2). From Lemma 3.2, Lemma 3.3, (4.2), and the triangle inequality, it is easy to derive (4.3) and (4.4). □

5. Numerical Experiments

In this section, we give a numerical example to demonstrate our theoretical results. Based on the above fully discrete CMFEM approximation scheme (2.12)-(2.18), we use the projection gradient algorithm to solve the OCPs (1.1). The projection $P_{K_h}: W_h \to K_h$, which satisfies: for any $w \in W_h$ find $P_{K_h} w \in K_h$ such that

$$
(P_{K_h} w - w, P_{K_h} w - w) = \min_{u \in K_h} (u - w, u - w).
$$

For an acceptable error Tol, we introduce the following projection gradient algorithm.

Algorithm 1. Projection gradient algorithm

- Step 1. Initialize $i = 1, y_{(i)}^0, z_{(i)}^N, u_{(i)}^n (n = 1, 2, \cdots, N)$;

- Step 2. For $n=1,2,\cdots,N$, solve the following system:

$$\begin{cases} \left(u^n_{(i+\frac{1}{2})},v\right)=\left(u^n_{(i)},v\right)-\rho_{(i)}\left(u^n_{(i)}-y^n_{(i)}p^{n-1}_{(i)},v\right), \quad \forall v\in K_h, \\ \left(\dfrac{y^n_{(i)}-\bar{y}^{n-1}_{(i)}}{k_n},w\right)+\left(\mathrm{div}\boldsymbol{p}^n_{(i)},w\right)+\left(u^n_{(i)}y^n_{(i)},w\right)=(f^n,w), \quad \forall w\in W_h, \\ \left(A^{-1}\boldsymbol{p}^n_{(i)},\boldsymbol{v}\right)-\left(y^n_{(i)},\mathrm{div}\boldsymbol{v}\right)=0, \quad \forall \boldsymbol{v}\in \boldsymbol{V}_h, \\ \left(\dfrac{z^{n-1}_{(i)}-\bar{\bar{z}}^n_{(i)}}{k_n},w\right)+\left(\mathrm{div}\boldsymbol{q}^{n-1}_{(i)},w\right)+\left(u^n_{(i)}z^{n-1}_{(i)},w\right)=\left(y^n_{(i)}-y^n_d,w\right), \quad \forall w\in W_h, \\ \left(A^{-1}\boldsymbol{q}^n_{(i)},\boldsymbol{v}\right)-\left(z^n_{(i)},\mathrm{div}\boldsymbol{v}\right)=-\left(\boldsymbol{p}^n_{(i)}-\boldsymbol{p}^n_d,\boldsymbol{v}\right), \quad \forall \boldsymbol{v}\in \boldsymbol{V}_h, \\ u_{(i+1)^n}=P_{K_h}(u^n_{(i+\frac{1}{2})}), \end{cases}$$

where we have omitted the subscript h and selected $\rho_{(i)}\in(0,1/4)$ in practice;

- Step 3. Compute the iterative error: $E_i=\sqrt{\sum_{n=1}^{N}k_n\|u^n_{(i+1)}-u^n_{(i)}\|^2}$;
- Step 4. If $E_i\le Tol$ or $i\ge 100$, stop; else $i=i+1$ go to Step 2;
- Step 5. Compute the errors of $|||u-u_h|||_{l^2(L^2)}$, $|||y-y_h|||_{l^\infty(L^2)}$, $|||\boldsymbol{p}-\boldsymbol{p}_h|||_{l^2(L^2)}$, $|||z-z_h|||_{l^\infty(L^2)}$, $|||\boldsymbol{q}-\boldsymbol{q}_h|||_{l^2(L^2)}$.

The numerical example was solved by Algorithm 1 with the C++ software package: AFEPack which is freely available [15]. Let $\Omega=[0,1]\times[0,1]$, $T=1$ and E be the 2×2 identity matrix.

Example 1. The data are as follows:

$$\begin{aligned} &\boldsymbol{b}=(1,1), A=\varepsilon\cdot E, \\ &y(x,t)=\sin(\pi t)x_1(1-2x_1)(1-x_1)\sin(2\pi x_2), \\ &\boldsymbol{p}(x,t)=-\varepsilon\begin{pmatrix}\sin(\pi t)(1-6x_1+6x_1^2)\sin(2\pi x_2)\\ 2\pi\sin(\pi t)x_1(1-2x_1)(1-x_1)\cos(2\pi x_2)\end{pmatrix}, \\ &z(x,t)=\sin(\pi(1-t))\sin(2\pi x_1)x_2(1-2x_2)(1-x_2), \\ &\boldsymbol{q}(x,t)=-\varepsilon\begin{pmatrix}2\pi\sin(\pi(1-t))\cos(2\pi x_1)x_2(1-2x_2)(1-x_2)\\ \sin(\pi(1-t))\sin(2\pi x_1)(1-6x_2+6x_2^2)\end{pmatrix}, \\ &u(x,t)=\max\{0,-z(x,t)\}, \\ &f(x,t)=y_t(x,t)+\boldsymbol{b}\cdot\nabla y(x,t)+\mathrm{div}\boldsymbol{p}(x,t)+u(x,t)y(x,t), \\ &y_d(x,t)=y(x,t)+z_t(x,t)+\boldsymbol{b}\cdot\nabla z(x,t)-\mathrm{div}\boldsymbol{q}(x,t)-u(x,t)z(x,t), \\ &\boldsymbol{p}_d(x,t)=\boldsymbol{p}(x,t)+\varepsilon\boldsymbol{q}(x,t)+\nabla z(x,t). \end{aligned}$$

For $\varepsilon=10^{-1}$ and $\varepsilon=10^{-3}$, the errors on a sequence of uniformly refined meshes's size h and time step size k are shown in Tables 1-2. It is easy to see that $|||u-u_h|||_{l^2(L^2)}=\mathscr{O}(h+k)$, $|||y-y_h|||_{l^\infty(L^2)}+|||\boldsymbol{p}-\boldsymbol{p}_h|||_{l^2(L^2)}=\mathscr{O}(h+k)$, and $|||z-z_h|||_{l^\infty(L^2)}+|||\boldsymbol{q}-\boldsymbol{q}_h|||_{l^2(L^2)}=\mathscr{O}(h+k)$. It is consistent with the previous convergence analysis results.

TABLE 1. Numerical results with $\varepsilon = 10^{-1}$, Example 1.

$h=k$	$\frac{1}{10}$	$\frac{1}{20}$	$\frac{1}{40}$	$\frac{1}{80}$
$\|\|\|u-u_h\|\|\|_{l^2(L^2)}$	6.3712e-02	3.1387e-02	1.6099e-02	8.3536e-03
$\|\|\|y-y_h\|\|\|_{l^\infty(L^2)}$	4.1573e-02	2.1174e-02	1.0793e-02	5.3782e-03
$\|\|\|\boldsymbol{p}-\boldsymbol{p}_h\|\|\|_{l^2(L^2)}$	8.9619e-02	4.3653e-02	2.2054e-02	1.0454e-02
$\|\|\|z-z_h\|\|\|_{l^\infty(L^2)}$	6.3702e-02	3.1379e-02	1.6101e-02	8.3538e-03
$\|\|\|\boldsymbol{q}-\boldsymbol{q}_h\|\|\|_{l^2(L^2)}$	1.0430e-01	5.2853e-02	2.5262e-02	1.3664e-02

TABLE 2. Numerical results with $\varepsilon = 10^{-3}$, Example 1.

$h=k$	$\frac{1}{10}$	$\frac{1}{20}$	$\frac{1}{40}$	$\frac{1}{80}$
$\|\|\|u-u_h\|\|\|_{l^2(L^2)}$	4.2618e-01	2.1311e-01	1.0609e-01	5.3044e-02
$\|\|\|y-y_h\|\|\|_{l^\infty(L^2)}$	2.4618e-01	1.2310e-01	5.1160e-02	2.5578e-02
$\|\|\|\boldsymbol{p}-\boldsymbol{p}_h\|\|\|_{l^2(L^2)}$	4.1896e-01	2.0952e-01	1.0478e-01	5.2391e-02
$\|\|\|z-z_h\|\|\|_{l^\infty(L^2)}$	3.6584e-01	1.8298e-01	9.1491e-02	4.5745e-02
$\|\|\|\boldsymbol{q}-\boldsymbol{q}_h\|\|\|_{l^2(L^2)}$	6.8645e-01	3.4332e-01	1.7167e-01	8.3583e-02

In Figure 1, we show the relationship between $\log_{10}(error)$ and $\log_{10}(node)$ and can see the convergence rate $\mathcal{O}(h+k)$, which is consistent with the theoretical results in Section 4.

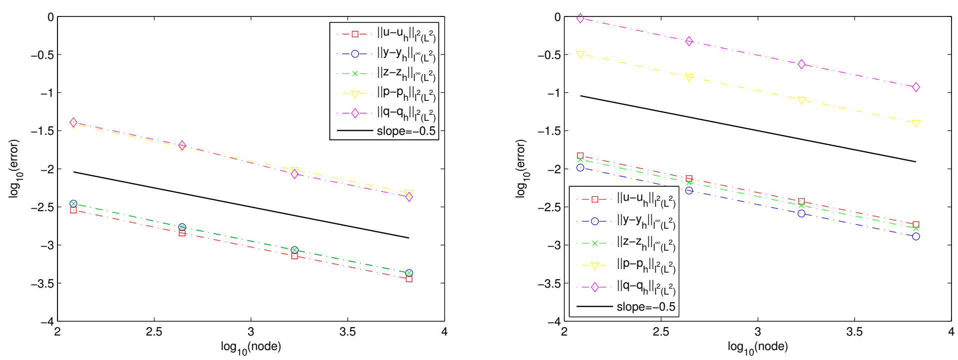

FIGURE 1. The convergence rate with $\varepsilon = 10^{-1}$ (left) and $\varepsilon = 10^{-3}$ (right).

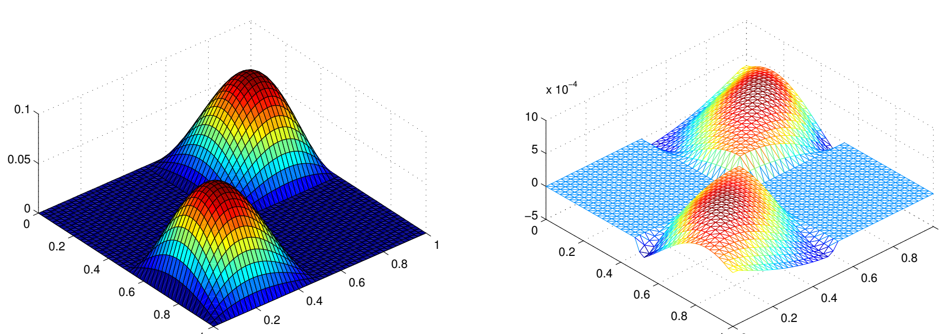

FIGURE 2. The exact solution u (left) at the error $u-u_h$ (right) $t = 0.5$ with $\varepsilon = 10^{-3}$.

In Figure 2, we show the profiles of the exact solution u (left) alongside the error $u-u_h$ (right) at $t=0.5$ with $h=k=\frac{1}{40}$ and $\varepsilon=10^{-3}$.

Funding

This work was supported by the National Natural Science Foundation of China (11401201), the Natural Science Foundation of Hunan Province (2020JJ4323), the Scientific Research Project of Hunan Provincial Department of Education (20A211), and the construct program of applied characteristic discipline in Hunan University of Science and Engineering.

References

[1] F. Brezzi, M. Fortin, Mixed and Hybrid Finite Element Methods, Springer-Verlag, Berlin, 1999.
[2] Y. Chang, D. Yang, Finite element approximation for a class of parameter estimation problems, J. Syst. Sci. Complex 27 (2014) 866-882.
[3] Y. Chen, Z. Lu, High Efficient and Accuracy Numerical Methods for Optimal Control Problems, Science Press, Beijing, 2015.
[4] Y. Chen, Y. Huang, W. Liu, N. Yan, Error estimates and superconvergence of mixed finite element methods for convex optimal control problems, J. Sci. Comput. 42 (2009) 382-403.
[5] Y. Chen, Z. Lu, Error estimates of fully discrete mixed finite element methods for semilinear quadratic parabolic optimal control problems, Comput. Meth. Appl. Mech. Eng. 199 (2010) 1415-1423.
[6] Y. Chen, Z. Lu, Y. Huang, Superconvergence of triangular Raviart-Thomas mixed finite element methods for bilinear constrained optimal control problem, Comput. Math. Appl. 66 (2013) 1498-1513.
[7] J. Douglas, T. Russell, Numercal methods for convection-dominated diffusion problems based on combining the method of charateristics with finite element or finite difference procedures, SIAM J. Numer. Anal. 19 (1982) 871-885.
[8] H. Fu, H. Rui, A priori error estimates for optimal control problems governed by transient advection-diffusion equations, J. Sci. Comput. 38 (2009) 290-315.
[9] H. Fu, A characteristic finite element method for optimal control problems governed by convection-diffusion equations, J. Comput. Appl. Math. 235 (2010) 825-836.
[10] H. Fu, H. Rui, Adaptive characteristic finite element approximation of convection-diffusion optimal control problems, Numer. Methods Partial Differential Equ. 29 (2013) 979-998.
[11] H. Fu, H. Rui, A characteristic-mixed finite element method for time-dependent convection-diffusion optimal control problem, Appl. Math. Comput. 218 (2011) 3430-3440.
[12] D. Gathungu, A. Borzì, A multigrid scheme for solving convection-diffusion-integral optimal control problems, Comput. Visual Sci. 22 (2019) 43-55.
[13] M. Hinze, R. Pinnau, M. Ulbrich, S. Ulbrich, Optimization with PDE Constraints, Springer-Verlag, Dordrecht, 2008.
[14] T. Hou, L. Chen, Y. Yang, et al., Two-grid Raviart-Thomas mixed finite element methods combined with Crank-Nicolson scheme for a class of nonlinear parabolic equations, Adv. Comput. Math. 46 (2020) 24.
[15] R. Li, W. Liu, The AFEPack Handbook, 2006, https://blog.csdn.net/HateCode/article/details/1413290.
[16] W. Liu, T. Tiba, Error estimates for the finite element approximation of a class of nonlinear optimal control problems, Numer. Funct. Optim. 22 (2001) 953-972.
[17] W. Liu, N. Yan, Adaptive Finite Element Methods for Optimal Control Governed by PDEs, Science Press, Beijing, 2008.
[18] J. Lions, Optimal Control of Systems Governed by Partial Differential Equations, Springer, Berlin, 1971.
[19] Z. Lu, F. Cai, J. Yang, et al., Optimal decision for multi-pollutants problem under ecological compensation mechanism and learning by doing, J. Clean. Prod. 359 (2022) 132010.
[20] Z. Lu, F. Cai, J. Yang, et al., Optimal control for transboundary pollution under inter-temporal transfer of emission permits: A differential game approach, Appl. Math. Model. 113 (2023) 376-379.
[21] Z. Lu, S. Zhang, L^∞-error estimates of rectangular mixed finite element methods for bilinear optimal control problem, Appl. Math. Comput. 300 (2017) 79-94.

[22] J. Rashidinia, M. Khasi, G. Fasshauer, A stable Gaussian radial basis function method for solving nonlinear unsteady convection-diffusion-reaction equations, Comput. Math. Appl. 75 (2018) 1831-1850.
[23] H. Rui, M. Tabata, A second order characteristic finite element scheme for convection-diffusion problems, Numer. Math. 92 (2002) 161-177.
[24] F. Samadi, A. Heydari, S. Effati, A numerical method based on a bilinear pseudo-spectral method to solve the convection-diffusion optimal control problems, Inter. J. Comput. Math. 98 (2021) 28-46.
[25] Y. Tang, Y. Hua, Adaptive variational discretization approximation method for parabolic optimal control problems, J. Inequal. Appl. 2020 (2020) 240.
[26] X. Tian, J. Lin, A novel radial basis function method for 3D linear and nonlinear advection diffusion reaction equations with variable coefcients, Eng. Comput. 38 (2022) 475–488.
[27] X. Xing, Y. Chen, Error estimates of mixed methods for optimal control problems governed by parabolic equations, Inter. J. Numer. Meth. Eng. 75 (2008) 735-754.
[28] X. Xiao, X. Feng, Y. He, Numerical simulations for the chemotaxis models on surfaces via a novel characteristic finite element method, Comput. Math. Appl. 78 (2019) 20-34.
[29] H. Yücel, M. Stoll, P. Benner, A discontinuous Galerkin method for optimal control problems governed by a system of convection-diffusion PDEs with nonlinear reaction terms, Comput. Math. Appl. 70 (2015) 2414-2431.